

Survival Concept-Based Learning Models

Stanislav R. Kirpichenko, Lev V. Utkin
Andrei V. Konstantinov, Natalya M. Verbova

Higher School of Artificial Intelligence Technologies
Peter the Great St.Petersburg Polytechnic University
St.Petersburg, Russia

e-mail: kirpich_sr@spbstu.ru, utkin_lv@spbstu.ru
konstantinov_av@spbstu.ru, verbova_nm@spbstu.ru

Abstract

Concept-based learning enhances prediction accuracy and interpretability by leveraging high-level, human-understandable concepts. However, existing CBL frameworks do not address survival analysis tasks, which involve predicting event times in the presence of censored data – a common scenario in fields like medicine and reliability analysis. To bridge this gap, we propose two novel models: SurvCBM (Survival Concept-based Bottleneck Model) and SurvRCM (Survival Regularized Concept-based Model), which integrate concept-based learning with survival analysis to handle censored event time data. The models employ the Cox proportional hazards model and the Beran estimator. SurvCBM is based on the architecture of the well-known concept bottleneck model, offering interpretable predictions through concept-based explanations. SurvRCM uses concepts as regularization to enhance accuracy. Both models are trained end-to-end and provide interpretable predictions in terms of concepts. Two interpretability approaches are proposed: one leveraging the linear relationship in the Cox model and another using an instance-based explanation framework with the Beran estimator. Numerical experiments demonstrate that SurvCBM outperforms SurvRCM and traditional survival models, underscoring the importance and advantages of incorporating concept information. The code for the proposed algorithms is publicly available.

Keywords: concept-based learning, survival analysis, neural networks, censored data, interpretation

1 Introduction

Concept-based learning (CBL) [1, 2, 3, 4, 5, 6] is an approach aimed at improving classification or regression accuracy. More importantly, it addresses the challenge of interpreting predictions generated by deep learning models [7, 8, 9]. Concepts represent semantic descriptions of input images and can be viewed as high-level, human-understandable attributes or abstractions [1, 10]. In most cases, concept labels are annotated by humans or domain experts [11]. Unlike conventional black-box models, which establish a direct relationship between input data and predictions, CBL models first predict concept values from the input data and then use these predicted concepts to determine target class labels [12].

One of the key architectures within the CBL framework is the concept bottleneck model (CBM), introduced by Koh et al. [12]. This model consists of two predictors: a concept predictor and a class predictor. The concept predictor explicitly generates concept labels from images, while the class predictor determines the final label based on these concept predictions. The concept predictor is typically implemented using a convolutional neural network (CNN), which extracts a feature vector encoding the concepts from the input image. The class predictor, often implemented as a downstream layer (usually a linear fully-connected layer), predicts the final class using only the predicted concepts. This downstream layer serves as a tool for interpreting the final class prediction in terms of the underlying concepts [13, 14]. Additionally, the CBM architecture allows for interactive intervention during the interpretation and prediction process [13]. The CBM and its numerous modifications, such as [15, 16, 17, 18, 19, 20], are considered some of the most notable representatives of CBL models.

An important type of data that arises in many fields, including medicine, reliability, safety, and economics, is event time data. Event time observations can be approached within the framework of conventional regression problems. However, unlike standard observations, some events may remain unobserved because they occur after a fixed time point. Such data is referred to as censored observations. Survival analysis [21] is a framework designed to handle two types of event time data: censored (where the event of interest is not observed) and uncensored (where the event of interest is observed). Unlike many traditional machine learning models, the predictions of survival models are typically expressed as probabilistic functions of time. For example, the survival function represents the probability of an event not occurring up to a predefined time point.

It is worth noting that Forest et al. [22] introduced a concept bottleneck model (CBM) for predicting the remaining useful life. In their work, concepts are represented by different degradation modes associated with the remaining useful life. However, this approach remains within the standard regression framework of CBMs and does not address censored data or incorporate survival analysis. To the best of our knowledge, no existing method combines concept-based learning (CBL) with survival analysis. Given

the importance of tasks involving interpretable predictions and improved prediction accuracy, we propose a novel approach that integrates survival analysis into the CBM framework. This model, called *SurvCBM* (**S**urvival **C**oncept-based **B**ottleneck **M**odel), is designed to address survival analysis tasks.

The first idea underlying the proposed approach is to implement the second predictor in the CBM as the Cox proportional hazards model [23], where concepts serve as covariates with a linear relationship between them. In this setup, the coefficients of the concept linear combination in the Cox model, along with the covariates, can be interpreted as measures of the concepts’ impact on the predictions. These predictions are expressed in terms of survival functions or other probabilistic measures within the survival analysis framework [24]. Alternatively, the second predictor can be implemented using the Beran estimator [25], which also provides a means to interpret predictions [26]. When using the Beran estimator, we can adopt an approach within the framework of example-based explanations. This approach involves selecting several instances from the training set that are closest to the explainable instance, based on the proximity of their predicted survival functions as measured by a distance metric. The importance of concepts in the prediction is then determined by the number of matching concepts between the closest instances and the explainable instance. The more concepts that coincide, the greater their significance in the prediction. This explanation approach is universal and can be applied to many survival models integrated into *SurvCBM* for predicting the probability distributions of event times.

The second idea behind the proposed approach involves two distinct architectures for CBL models. The primary architecture is a CBM with a bottleneck layer consisting of concept logits, followed by either the Beran or Cox models. The secondary architecture, introduced for comparison purposes, also employs the Beran or Cox models but uses concepts as regularization to enhance prediction accuracy. This architecture is referred to as *SurvRCM* (**S**urvival **R**egularized **C**oncept-based **M**odel). Both neural network architectures are trained in an end-to-end manner.

Our contributions can be summarized as follows:

1. New concept-based survival models, *SurvCBM* and *SurvRCM*, are proposed for dealing with censored data in the framework of survival analysis. These models not only improve the accuracy of predictions but also provide a tool for interpreting these predictions in terms of concepts. The models are based on the Cox proportional hazards model and the Beran estimator.
2. Two approaches for interpreting the predicted survival functions are considered, depending on the survival model used in *SurvCBM* or *SurvRCM*. The first approach is based on the assumption of a linear relationship between covariates in the Cox model. Using the trained regression coefficients and the logits of the concepts corresponding to the explainable instance, the importance of each concept is

determined by its contribution to the linear combination of covariates. The second approach is based on comparing instances and their concepts, focusing on those with survival functions closest to the survival function of the new explainable instance. The importance of concepts is determined by the frequency of matching concepts between the closest instances and the explainable instance.

3. The proposed models are compared with each other and with a survival model that does not incorporate concepts.
4. Various numerical experiments are conducted to compare the proposed concept-based survival models under different conditions. The results demonstrate that the first architecture, SurvCBM, outperforms the other models. Moreover, they demonstrate the importance and advantage of applying concept information. The corresponding codes implementing the proposed models are publicly available at: <https://github.com/NTAILab/SurvCBM>.

The paper is organized as follows. Related work considering the existing explanation methods can be found in Section 2. A short description of basic concepts of survival analysis, including the Cox model and the Beran estimator, as well as concept-based learning is given in Section 3. A general idea of the concept-based survival models is provided in Section 4. Numerical experiments comparing different architectures of the survival models are given in Section 5. Approaches to interpreting predictions of concept-based survival models are studied in Section 6. Concluding remarks are provided in Section 7.

2 Related work

Concept-based learning models. Many CBL models were proposed in recent years [2, 27, 6] in order to improve the classification and regression performance of machine learning models and to interpret their predictions in terms of the high-level concepts. A large part of the models are CBMs [12] which have attracted special attention due to a number of remarkable properties. In particular, we point out stochastic CBMs [19], interactive CBMs [13], editable CBMs [11], semi-supervised CBMs [28], probabilistic CBMs [15], label-free CBMs [29], CBMs without predefined concepts, [30] [31], post-hoc CBMs [32], incremental residual CBMs [33], concept bottleneck generative models [16], any CBMs [34]. concept complement bottleneck models [30]. The above CBMs are a small part of various CBL models proposed in literature.

Concept-based models, their advantages and disadvantages are considered in the survey papers [1, 10, 35, 36, 37].

Survival analysis in machine learning. Many survival machine learning models have been developed [38] due to their importance in several application areas, for example, in medicine, safety, reliability, economics. Detailed reviews of many survival models can be found in [38, 39, 40]. Deep survival machine learning models were reviewed in [41]. A practical introduction to survival analysis was provided by Emmert-Streib and Dehmer in [42].

A large part of survival models can be regarded as extensions of conventional machine learning models under condition of censored data. For example, several survival models are based on applying neural networks and deep learning [41, 43, 44, 45, 46, 47, 48, 49, 50], several survival models are based on the transformer architectures [51, 52, 53, 54, 55, 56, 57], attention-based deep survival models were proposed in [58, 59]. A part of models is based on extending the random forest [60, 61]. Convolutional neural networks also used in survival analysis [62]. Many machine learning survival models extend the Cox model [23]. They mainly relax or modify the linear relationship assumption used in the Cox model [63, 64].

Despite the intensive development of survival models, their application to concept-based learning is currently not reflected in the literature. Therefore, this work can be considered as the first attempt to create a survival concept-based model.

3 Background

3.1 Formal problem statement of concept-based learning

In the conventional supervised concept-based model setting, a training set consists of triplets $(\mathbf{x}_i, y_i, \mathbf{c}_i)$, $i = 1, \dots, n$, where $\mathbf{x}_i \in \mathbb{R}^D$ or $\mathbf{x}_i \in \mathbb{R}^{d_1 \times d_2}$ is the input instance represented as a vector or a matrix; $y_i \in \mathcal{Y} = \{1, \dots, s\}$ is the corresponding target defining s -class classification task; $\mathbf{c}_i = (c_i^{(1)}, \dots, c_i^{(m)}) \in \mathcal{C}$ is a vector of m high-level concepts which describe the i -th instance \mathbf{x}_i with $c_i^{(j)} \in \{0, \dots, k_j - 1\}$; k_j is the number of the j -th concept values. Concepts are usually represented as a vector consisting of binary elements such that the j -th unit element corresponds to the case when the j -th concept is presented in the description of the i -th instance. The main task of CBL is to construct a machine learning models (a classifier or a regressor) $h : \mathbb{R}^D \rightarrow (\mathcal{C}, \mathcal{Y})$ to predict concepts and the target for a new input instance \mathbf{x} .

Another task is to explain the predicted target in terms of concepts. One of the approaches for solving this task is the CBM proposed by Koh et al. [12], which consists of two parts: the first part explicitly predicts concept labels from instances and implements the map $g : \mathcal{X} \rightarrow \mathcal{C}$, the second part predicts the target class using only predicted concepts and implements the map $f : \mathcal{C} \rightarrow \mathcal{Y}$. The vector of concepts \mathbf{c} or their probabilities (logits) predicted by the first part can be viewed as a bottleneck. As a result, the target class y of a new input instance \mathbf{x} is defined as $y = f(g(\mathbf{x}))$.

3.2 Elements of survival analysis

Instances in survival analysis are represented by a triplet $(\mathbf{x}_i, \delta_i, T_i)$, where $\mathbf{x}_i^T = (x_i^{(1)}, \dots, x_i^{(d)}) \in \mathbb{R}^d$ is a vector of d features characterizing the i -th instance whose time to an event of interest is T_i ; δ_i is the censoring indicator taking the value 1 if the event of interest is observed at time T_i (uncensored observation), and 0 if the event is not observed (censored observation) [21]. For censored observations, it is only known that the time to the event exceeds the duration of observation. Survival analysis aims to estimate the time to the event T for a new instance \mathbf{x} by using the training set $\mathcal{A} = \{(\mathbf{x}_i, \delta_i, T_i), i = 1, \dots, n\}$.

One of the important elements of survival analysis is the survival function (SF) denoted as $S(t | \mathbf{x})$, which is the probability of surviving beyond time t , that is $S(t | \mathbf{x}) = \Pr\{T > t | \mathbf{x}\}$. Another element is the cumulative hazard function (CHF) denoted as $H(t | \mathbf{x})$ an expressed through the SF as follows:

$$S(t | \mathbf{x}) = \exp(-H(t | \mathbf{x})). \quad (1)$$

Another element of survival analysis used for comparison of different survival models is the C-index [65]. It estimates the probability that event times of a pair of instances are correctly ranking. Let \mathcal{J} be a set of all pairs (i, j) satisfying conditions $\delta_i = 1$ and $T_i < T_j$. The C-index is formally computed as [66, 38]:

$$C = \frac{\sum_{(i,j) \in \mathcal{J}} \mathbf{1}[\widehat{T}_i < \widehat{T}_j]}{\sum_{(i,j) \in \mathcal{J}} 1}, \quad (2)$$

where \widehat{T}_i and \widehat{T}_j are expected (predicted) event times obtained from the predicted SFs $S(t | \mathbf{x}_i)$ and $S(t | \mathbf{x}_j)$.

A popular semi-parametric regression model for analysis of survival data is the Cox proportional hazards model that calculates the effects of observed covariates on the risk of an event occurring [23]. The model assumes that the log-risk of an event of interest is a linear combination of covariates or features. According to the Cox model, the CHF at time t given instance \mathbf{x} is defined as:

$$H(t | \mathbf{x}, \mathbf{b}) = H_0(t) \exp(\mathbf{b}^T \mathbf{x}), \quad (3)$$

where $H_0(t)$ is the baseline CHF estimated by using the Nelson–Aalen estimator [21, 42]; $\mathbf{b}^T = (b_1, \dots, b_m)$ is a vector of the model parameters in the form of the regression coefficients which can be found by maximizing the partial likelihood function for the dataset \mathcal{A} .

The SF $S(t | \mathbf{x}, \mathbf{b})$ in the framework of the Cox model is computed as

$$S_C(t | \mathbf{x}, \mathbf{b}) = (S_0(t))^{\exp(\mathbf{b}^T \mathbf{x})}. \quad (4)$$

Here $S_0(t)$ is the baseline SF which is also determined by using the Nelson–Aalen estimator. It is important to note that functions $H_0(t)$ and $S_0(t)$ do not depend on \mathbf{x} and \mathbf{b} .

Another important model which is used below is the Beran estimator [25] which estimates the SF on the basis of the dataset \mathcal{A} as follows:

$$S_B(t | \mathbf{x}) = \prod_{t_i \leq t} \left\{ 1 - \frac{\alpha(\mathbf{x}, \mathbf{x}_i)}{1 - \sum_{j=1}^{i-1} \alpha(\mathbf{x}, \mathbf{x}_j)} \right\}^{\delta_i}, \quad (5)$$

where time moments t_1, \dots, t_n are ordered; the weight $\alpha(\mathbf{x}, \mathbf{x}_i)$ conforms with relevance of the i -th instance \mathbf{x}_i to the vector \mathbf{x} and can be defined by using kernels $K(\mathbf{x}, \mathbf{x}_i)$ as

$$\alpha(\mathbf{x}, \mathbf{x}_i) = \frac{K(\mathbf{x}, \mathbf{x}_i)}{\sum_{j=1}^n K(\mathbf{x}, \mathbf{x}_j)}. \quad (6)$$

In particular, if to use the Gaussian kernel with the parameter τ , then weights $\alpha(\mathbf{x}, \mathbf{x}_i)$ are of the form:

$$\alpha(\mathbf{x}, \mathbf{x}_i) = \text{softmax} \left(-\frac{\|\mathbf{x} - \mathbf{x}_i\|^2}{\tau} \right). \quad (7)$$

The Beran estimator is reduced to the Kaplan–Meier estimator [38] when all weights are identical, i.e., $\alpha(\mathbf{x}, \mathbf{x}_i) = 1/n$ for all $i = 1, \dots, n$.

4 Description of concept-based survival models

4.1 Concept-based survival problem statement

In the survival concept-based learning setting, a training set \mathcal{A} is represented by a set of n quadruplets $(\mathbf{x}_i, \mathbf{c}_i, T_i, \delta_i)$, $i = 1, \dots, n$, which combines concept-based and survival information considered above. Unlike most concept-based learning models, predictions in the survival CBL are SFs $S(t | \mathbf{x}, \mathbf{c})$ or CHFs $H(t | \mathbf{x}, \mathbf{c})$. For simplicity, we will consider only SFs because CHFs are expressed through the corresponding SFs. The concept-based survival analysis aims to estimate the SF $S(t | \mathbf{x})$ as well as the concept vector \mathbf{c} for a new instance \mathbf{x} by using the training set \mathcal{A} . Other elements of survival analysis, for example, the mean time to event, can be calculated on the basis of the SF. If we denote the set of SFs as \mathcal{S} , then our task is to construct machine learning models which implement the map $G : \mathbb{R}^D \rightarrow (\mathcal{C}, \mathcal{S})$. Two models are proposed and compared in this work.

4.2 The first model: SurvCBM

The second proposed model is derived from the architecture of the CBM. Its mathematical formulation can be expressed as follows:

$$S(t | \mathbf{x}, \mathcal{A}) = F(G(\mathbf{x})), \quad (8)$$

where $S(t | \mathbf{x}, \mathcal{A})$ is the SF obtained for a feature vector \mathbf{x} using training set \mathcal{A} ; $F(\mathbf{c})$ is a survival model defined over the concept space; $G(\mathbf{x})$ is a neural network (or a set of neural networks) that predicts the vector of concepts for the feature vector \mathbf{x} .

The architecture of the model is illustrated in Fig. 1. It can be seen from Fig. 1 that the input image \mathbf{x} is processed by a set of m convolutional neural networks (CNN-1, ..., CNN- m) where each network outputs a vector of concept logits $\mathbf{p}_i = (p_{i,1}, \dots, p_{i,k_i})$. Here, it is assumed that the i -th concept can take k_i possible values. The use of CNNs is crucial for reducing the dimensionality of the images and enabling the training of Cox or Beran models on lower-dimensional vectors. In SurvCBM, the Cox model and the Beran estimator are trained on the concatenated logits

$$\mathbf{p} = (\mathbf{p}_1, \dots, \mathbf{p}_m) = (p_{i,1}, \dots, p_{i,k_i}, i = 1, \dots, m) \in \mathbb{R}^M, \quad M = \sum_{i=1}^m k_i. \quad (9)$$

This is a very important peculiarity of SurvCBM, as it achieves a balance between two objectives: accurately defining the concept values and computing the SF. Furthermore, this design ensures that the model remains interpretable, and the computed SF can be explained in terms of the underlying concepts.

The general form of the loss function is given by:

$$\mathcal{L} = -\alpha \mathcal{L}_{\text{surv}} + (1 - \alpha) \mathcal{L}_{\text{CE}}, \quad (10)$$

where $\alpha \in (0, 1)$ is a hyperparameter.

The term \mathcal{L}_{CE} corresponds to solving the concept classification task. For a single data point \mathbf{x} with true concept values (y_1, \dots, y_m) , it is defined as:

$$\mathcal{L}_{\text{CE}} = -\frac{1}{m} \sum_{i=1}^m \log \frac{\exp(p_{i,y_i})}{\sum_{j=1}^{k_i} \exp(p_{i,j})}. \quad (11)$$

The term $\mathcal{L}_{\text{surv}}$ corresponds to solving the survival analysis task. To implement We apply $\mathcal{L}_{\text{surv}}$, we use the smoothed C-index function. For data points $\mathbf{x}_1, \dots, \mathbf{x}_n$ with true event times T_1, \dots, T_n , censoring indicators $\delta_1, \dots, \delta_n$ and estimated expected event times $\hat{T}_1, \dots, \hat{T}_n$, the loss function can be expressed as:

$$\mathcal{L}_{\text{surv}} = \frac{\sum_{i,j} \mathbb{I}_{T_j < T_i} \cdot \sigma(\hat{T}_i - \hat{T}_j) \cdot \delta_j}{\sum_{i,j} \mathbb{I}_{T_j < T_i} \cdot \delta_j}, \quad (12)$$

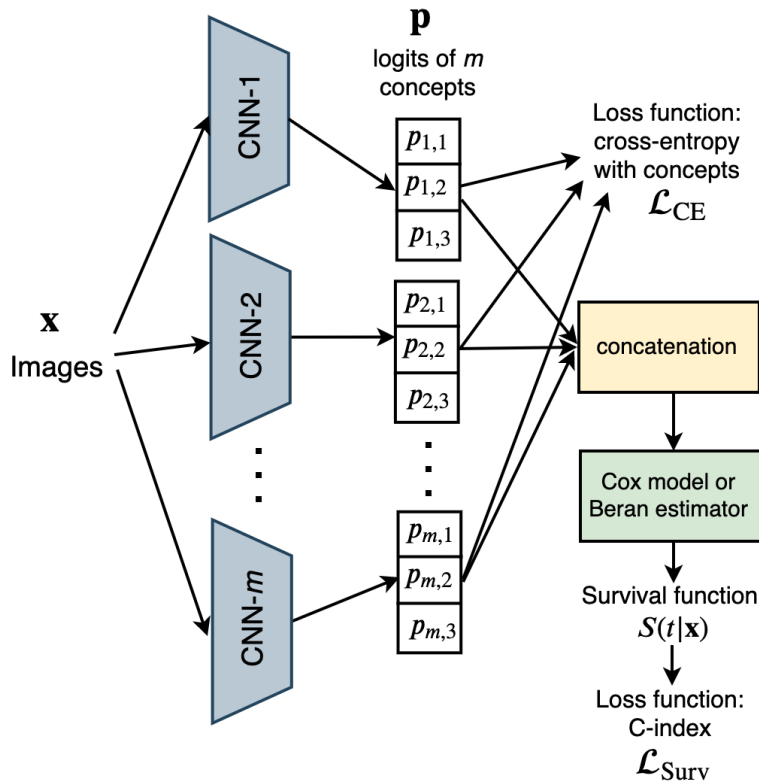


Figure 1: The architecture of SurvCBM

where σ is the sigmoid function with a temperature parameter ω , which is treated as a hyperparameter.

The loss function \mathcal{L}_{CE} is averaged over a batch during the optimization process, while the smoothed C-index is computed over all instances in the batch.

SurvCBM is trained in an end-to-end manner. It is worth noting that the use of a set of convolutional neural networks is one possible implementation of the model. Alternatively, a single network could be used to compute the vector \mathbf{p} of logits. However, our numerical experiments have demonstrated that using a set of networks yields more robust results.

4.3 The second model: SurvRCM

The SurvRCM does not follow the architecture of the CBM because it lacks a bottleneck layer. Nevertheless, we consider SurvRCM as a simplified variant of concept-based

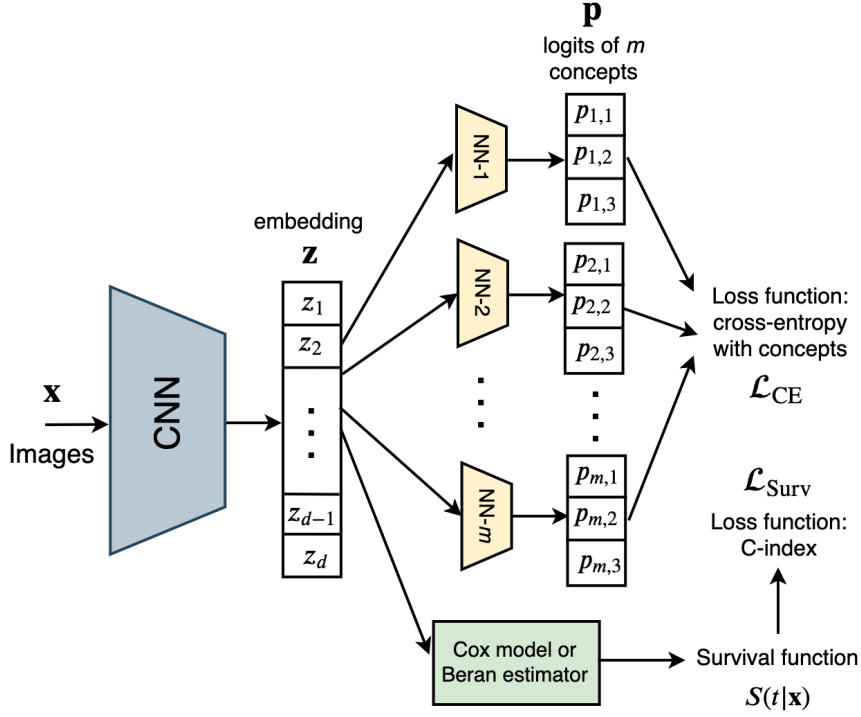


Figure 2: The architecture of SurvRCM

survival models. Its architecture is illustrated in Fig. 2. It can be seen from Fig. 2 that SurvRCM addresses the survival analysis task using concept information but without the bottleneck scheme. In this model, a CNN generates an embedding $\mathbf{z} \in \mathbb{R}^d$, which is fed to the Cox or Beran models to produce the SF $S(t | \mathbf{x})$. The CNN is again used to reduce the dimensionality of images and to learn the Cox or Beran models on lower-dimensional vectors. The embedding \mathbf{z} is also passed to a set of fully connected neural networks (NN-1,...,NN- m) to obtain the logits for m concepts. Each network produces a vector of logits for the i -th concept $\mathbf{p}_i = (p_{i,1}, \dots, p_{i,k_i})$, $i = 1, \dots, m$. Consequently, the Cox model or the Beran estimator are trained on the embeddings \mathbf{z} , but concepts are trained on logits \mathbf{p} .

The loss function for training SurvRCM is identical to that of SurvCBM, as given in (10). However, unlike SurvCBM, the term \mathcal{L}_{Surv} is computed under condition that the survival models (the Cox and Beran models) are trained on embeddings \mathbf{z} , but not on the vector of logits \mathbf{p} as in SurvCBM. The model is also trained in an end-to-end manner.

The main drawback of the SurvRCM model is that the loss function \mathcal{L}_{CE} acts as

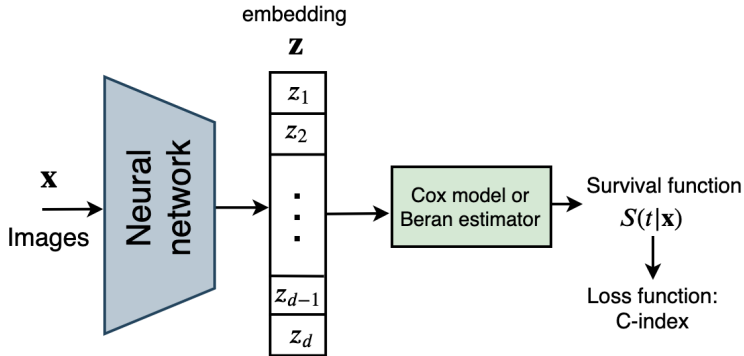


Figure 3: An architecture of SurvBase

a regularization term. It constrains the logits of the concepts \mathbf{p} , but does not directly influence the embeddings \mathbf{z} . As a result, the SF may be learned inaccurately, as it is derived from the embeddings rather than the concept logits. This limitation prevents the model from being fully interpretable, as the obtained concepts do not directly explain the SF.

5 Numerical Experiments

Two types of numerical experiments are conducted. The first type evaluates the performance of the proposed models, while the second type demonstrates their explanation mechanisms.

To assess the model performance, we compare the proposed models with each other and with a baseline survival model. Due to the absence of known survival CBMs, we compare the proposed models with a baseline model that solves the same survival analysis task without incorporating concept data. This comparison allows us to study the importance of correctly selected concepts for solving survival tasks when the input instances are images. In the baseline model, denoted as *SurvBase*, a CNN generates an embedding \mathbf{z} , which is used to train either the Cox model or the Beran estimator. The model is trained in an end-to-end manner, and its loss function consists solely of the term $\mathcal{L}_{\text{surv}}$, as defined in (12). The architecture of SurvBase is illustrated in Fig. 3. It can be seen from Fig. 3 that an image \mathbf{x} is fed into the CNN to produce an embedding $\mathbf{z} \in \mathbb{R}^d$. The Cox or Beran model is then applied to the set of embeddings to generate the SF $S(t | \mathbf{x})$.

The following model components and hyperparameters are used: the temperature ω of the sigmoid function in the smoothed C-index; parameter α in the loss function;

the number of instances in the background set of the Beran estimator; the parameter τ of the Gaussian kernel in the Beran estimator; the number of tasks, generated on each training epoch; the number of epochs; the optimizer and its parameters, including learning rate and weight decay; the size d of the embedding \mathbf{z} . Different values of the hyperparameters are tested, choosing those leading to the best results.

Experiments are conducted in two directions: comparison of the model performance depending on the number of training instances and depending on the number of uncensored data. The performance measures for comparison of the models are C-index, characterizing the survival model, and F1-measure, characterizing the concept classification accuracy. At that, values of the F1-measures indicated on graphs below are averaged over all concepts for brevity.

The cross-validation in all experiments is performed with 100 repetitions. Intervals on the graphs are the average value of these repetitions and the standard deviation.

5.1 Datasets

We consider the following composite images constructed from the datasets MNIST and CIFAR-10 with synthetically generated concepts and target event times:

1. **MNIST**. First, we apply MNIST dataset which is a commonly used large dataset of 28×28 pixel handwritten digit images [67]. It has a training set of 60,000 instances, and a test set of 10,000 instances. The dataset is available at <http://yann.lecun.com/exdb/mnist/>. To construct the concept-based MNIST dataset, images from the original MNIST dataset are combined into sets of four different digits. Each digit in its position defines a separate concept, where the concept's value corresponds to the digit itself. As a result, each data point in the dataset is described by four concepts, each taking one of 10 possible values. The event time is generated according to the Weibull distribution and is computed as follows:

$$T = \left(-\frac{\ln(u)}{\lambda \exp(\mathbf{b}^T \mathbf{c})} \right)^{\frac{1}{\nu}}, \quad (13)$$

where $u \sim U(0, 1)$ is the uniform random variable, \mathbf{c} is the vector of concepts; ν and λ are parameters of the Weibull distribution.

The generation parameters are $\mathbf{b}^T = (0.5, 1.5, -1, 0.001)$, $\nu = 2$, $\lambda = 10^{-4}$. Values of the censoring indicator δ are generated in accordance with the Bernoulli distribution. Examples of the generated instances as well as vectors of concepts \mathbf{c} are shown in Fig. 4.

2. **MNIST-sin**. The second dataset is identical to the first one, but the event times are generated using a probability distribution different from the Weibull distribu-

tion. The event times are generated according to the following formula:

$$T = \left(-\frac{\ln(u)}{\lambda(\sin(\mathbf{b}^T \mathbf{c}) + 1.001)} \right)^{\frac{1}{\nu}}, \quad (14)$$

where the generation parameters are $\mathbf{b}^T = (0.5, 1.5, -1, 0.001)$, $\nu = 4$, $\lambda = 0.01$.

3. **CIFAR-10.** The third dataset consists of four images from the well-known CIFAR-10 dataset [68], which contains 60,000 color images 32×32 drawn from 10 categories (50,000 training and 10,000 test images each). The dataset is available at <https://www.cs.toronto.edu/~kriz/cifar.html>. The following concepts vector of instances consisting of four CIFAR-10 images is used: (1 - number of animals, 2 - number of vehicles, 3 - number of flying objects, 4 - is there a cat on the picture). Concepts 1, 2, 3 take five values, the last one is binary. The event time is generated according to the Weibull distribution in the same way as for the MNIST dataset. The generation parameters are $\mathbf{b} = (-0.7, 1.5, -2, 5)$, $\nu = 2$, $\lambda = 0.01$. Examples of the dataset can be found in Fig. 5. As an example, it can be seen from the first instance in Fig. 5 that it contains three animals, one vehicle, no flying objects, and there is a cat. This implies that the corresponding vector of concepts is (3, 1, 0, 1).

5.2 MNIST dataset

First, we conduct numerical experiments using a synthetic dataset derived from the MNIST dataset. All metrics presented in the graphs are computed on the test set, which comprises 40% of the instances from the dataset. For experiments involving varying sample sizes, we set the proportion of uncensored instances to 33%.

First, we study how the sample size n impacts the accuracy (the C-index) of the models. Fig. 6 illustrates how the C-index of the compared models depends on the number of training instances n , when the Beran estimator (the left graph) and the Cox model (the right graph) are used as the survival models. It can be seen from the both graphs in Fig. 6 that SurvCBM outperforms the other models. It is interesting to point out that the most impressive results are demonstrated when the Cox model is used. This is due to the relatively simple feature space and the Weibull distribution used for generating the event times. It is also interesting to note that SurvRCM provides worse results even in comparison with SurvBase. We can also observe that the C-index of SurvBase is much smaller than that of SurvCBM. This implies that the concept information may significantly improve the model performance.

If the C-index characterizes the performance of models as survival models, then F1-measure characterizes the concept classification accuracy. Fig. 7 shows how the F1-measures of the models depend on the number of training instances under the same

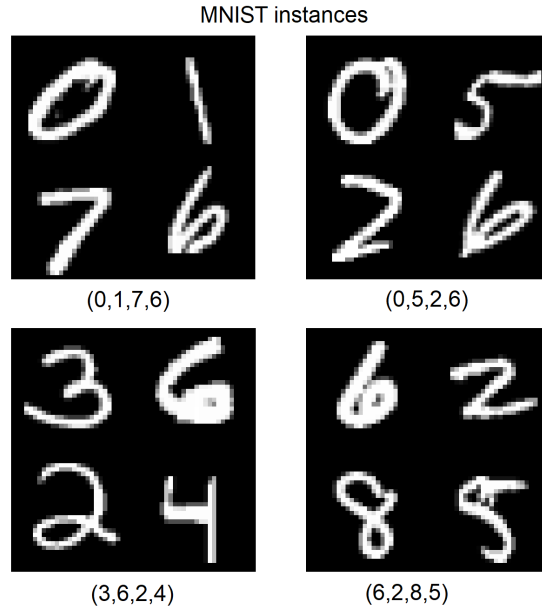


Figure 4: Instances constructed from the MNIST dataset; the corresponding concepts are denoted under the pictures in accordance with digits



Figure 5: Instances constructed from the CIFAR-10 dataset; the corresponding concepts are denoted under the pictures in accordance with their meanings

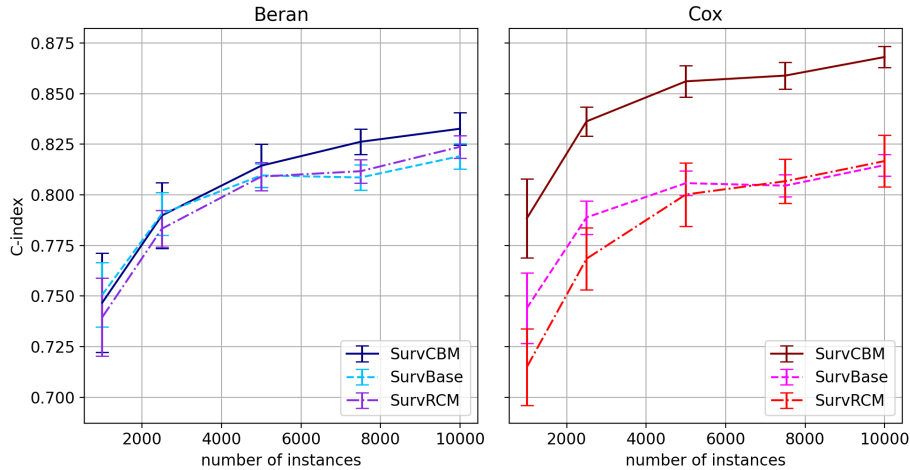


Figure 6: Dependencies of the survival model performance (the C-index) on the number of training instances for the Beran estimator (the left graph) and the Cox model (the right graph) when the MNIST dataset is used

conditions. We consider only two models because SurvBase does not deal with concepts. It can be seen from Fig. 7 that SurvCBM significantly outperforms the Mixture model. Moreover, results for SurvCBM for different survival models (the Beran and Cox models) are almost the same. It is important to note that the variance of SurvCBM results is extremely small compared with the variance of SurvRCM results. This fact illustrates a high robustness of SurvCBM.

The next question is how the model performance depends on the proportion of uncensored data ρ . Figs. 8 and 9 address this question. In particular, Fig. 8 shows that the C-index of SurvCBM significantly exceeds that of other models when the Cox model is used as the survival model. This can be explained by the fact that the Weibull distribution is used for generating the event times. One can also see from Fig. 8 that SurvBase provides unsatisfactory results. This fact again demonstrates that concept information may significantly improve the model performance. Fig. 9 is similar to Fig. 7. The F1-measure of SurvCBM weakly depends on the survival models, whereas SurvRCM strongly depends on both the survival models and the parameter ρ .

5.2.1 MNIST-sin

Let us study the model performance when the models are trained on the MNIST-sin dataset. In this dataset, the Weibull distribution of the event times is violated, and the proportionality of risk is also violated. The consequences of these violation are clearly seen from Fig. 10 where the Beran estimator demonstrates superior results compared

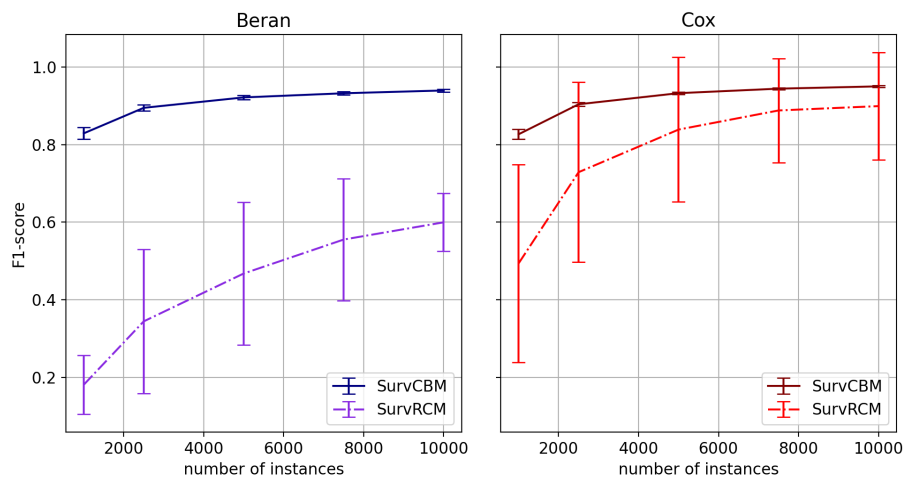


Figure 7: Dependencies of the concept classification performance (the F1-measure) on the number of training instances for the Beran estimator (the left graph) and the Cox model (the right graph) when the MNIST dataset is used

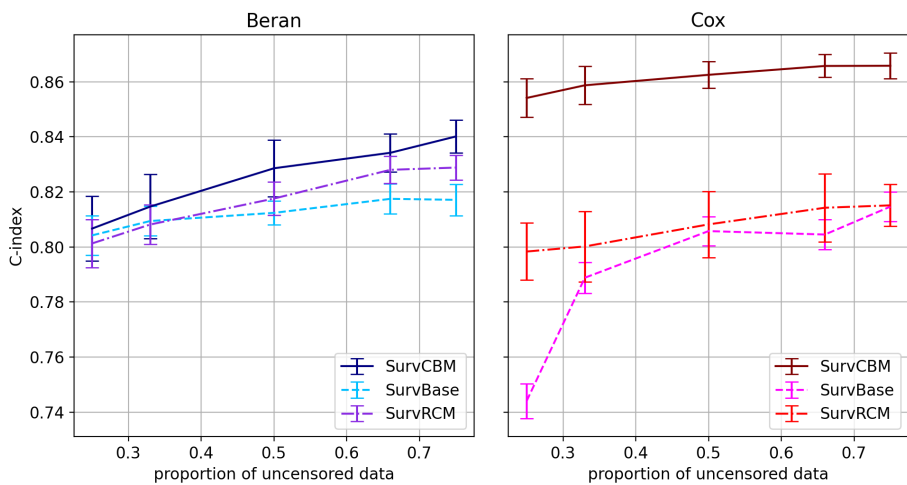


Figure 8: Dependencies of the survival model performance (the C-index) on the proportion of uncensored data for the Beran estimator (the left graph) and the Cox model (the right graph) when the MNIST dataset is used

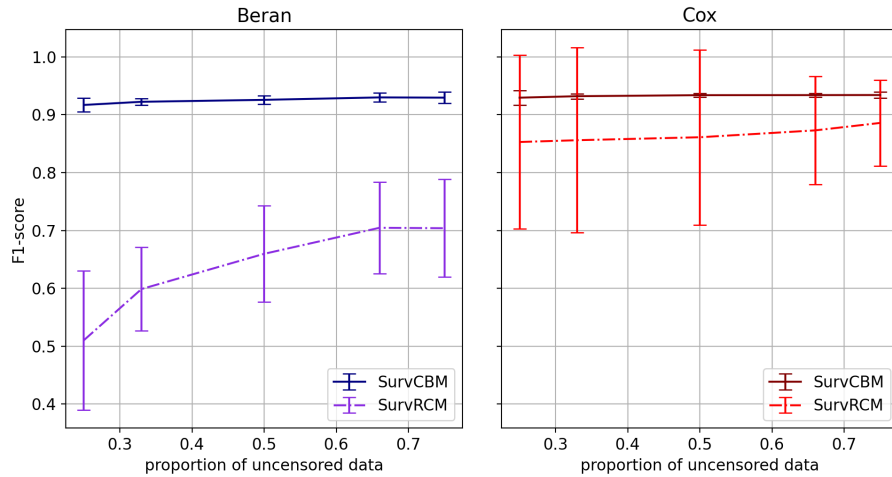


Figure 9: Dependencies of the survival model performance (the F1-measure) on the proportion of uncensored data for the Beran estimator (the left graph) and the Cox model (the right graph) when the MNIST dataset is used

to the Cox model when SurvCBM is used. This is because the Beran model effectively handles complex data structures by taking into account relationships between instances. It is interesting to note that all models have similar C-indices when the Cox model is used. Moreover, increasing the number of training instances does not significantly improve the performance of any of the models.

Fig. 11 shows how the F1-measures of the models depend on the number of training instances. It can be seen from Fig. 11 that SurvCBM outperforms SurvRCM for both the Beran estimator and the Cox model. We again observe that the F1-measures for both models, using either the Beran or Cox models, are almost the same.

Results depicted in Figs. 12 and 13 are consistent with the similar results shown in Figs. 10 and 11, respectively. We again observe that the C-index increases with the number of training instances. However, this increase is observed only for SurvCBM when the Beran estimator is used. At the same time, there is almost no improvement in the concept classification performance (the F1-measure) as the proportion of uncensored observations increases (see Fig. 13).

5.2.2 CIFAR-10

Similar numerical experiments are performed with the CIFAR-10 dataset. Figs. 14 and 15 demonstrate that the more complex data structure and principles of concept formation lead to worse results. The complex structure of the dataset does not allow satisfactory results to be obtained using the Cox model, even when the Weibull distribution is used

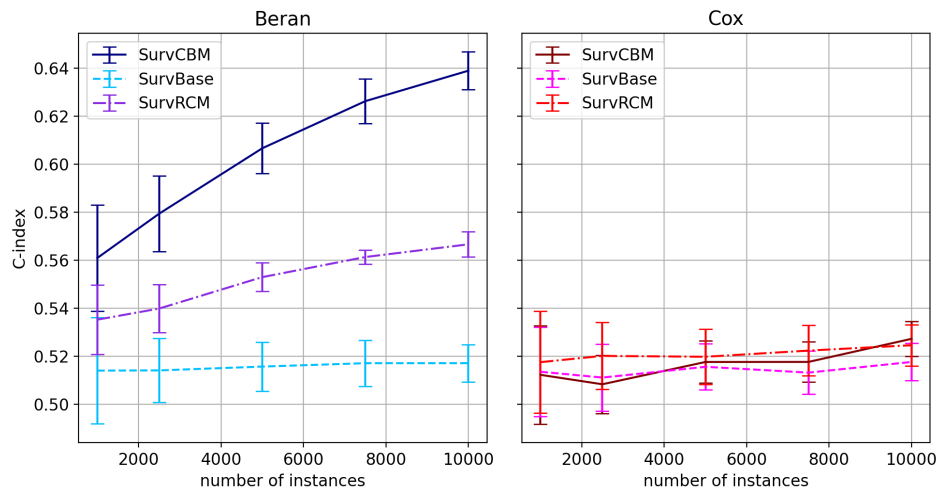


Figure 10: Dependencies of the survival model performance (the C-index) on the number of training instances for the Beran estimator (the left graph) and the Cox model (the right graph) when the MNIST-sin dataset is used

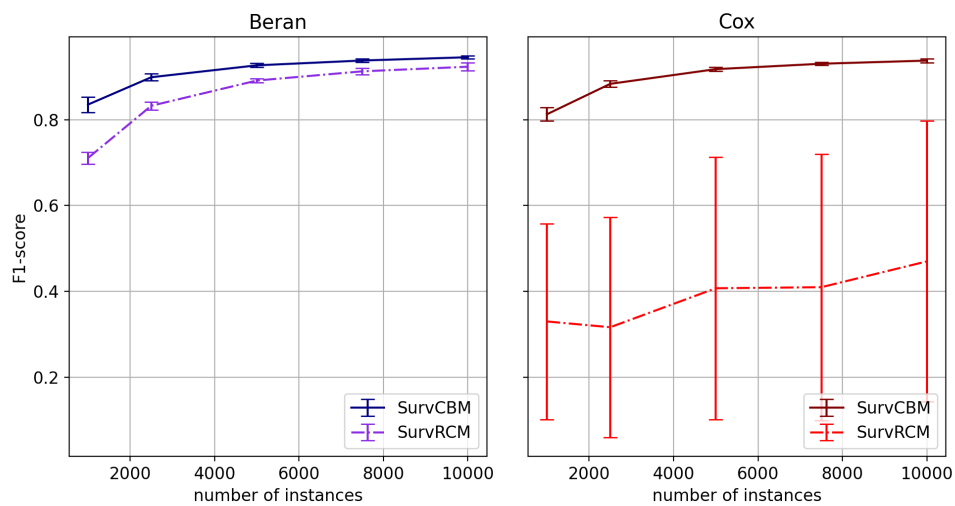


Figure 11: Dependencies of the survival model performance (the F1-measure) on the number of training instances for the Beran estimator (the left graph) and the Cox model (the right graph) when the MNIST-sin dataset is used

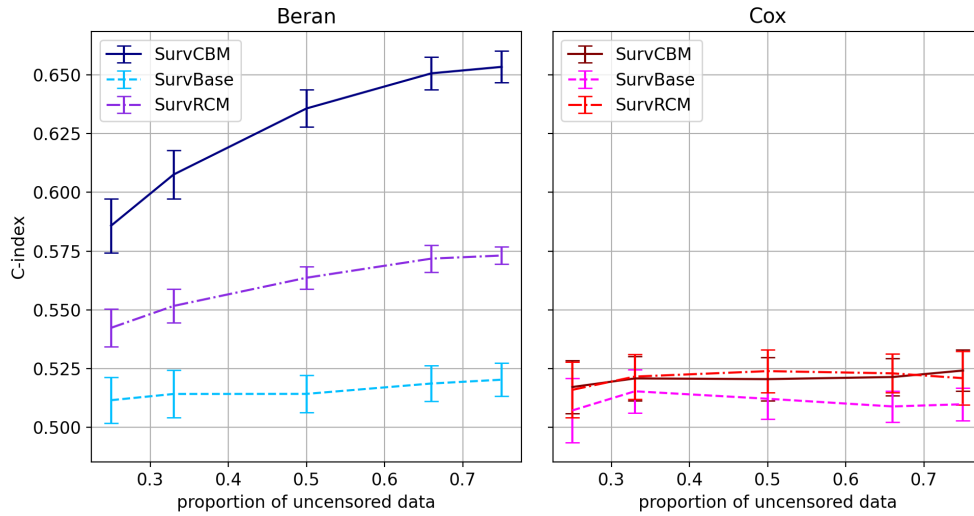


Figure 12: Dependencies of the survival model performance (the C-index) on the proportion of uncensored data for the Beran estimator (the left graph) and the Cox model (the right graph) when the MNIST-sin dataset is used

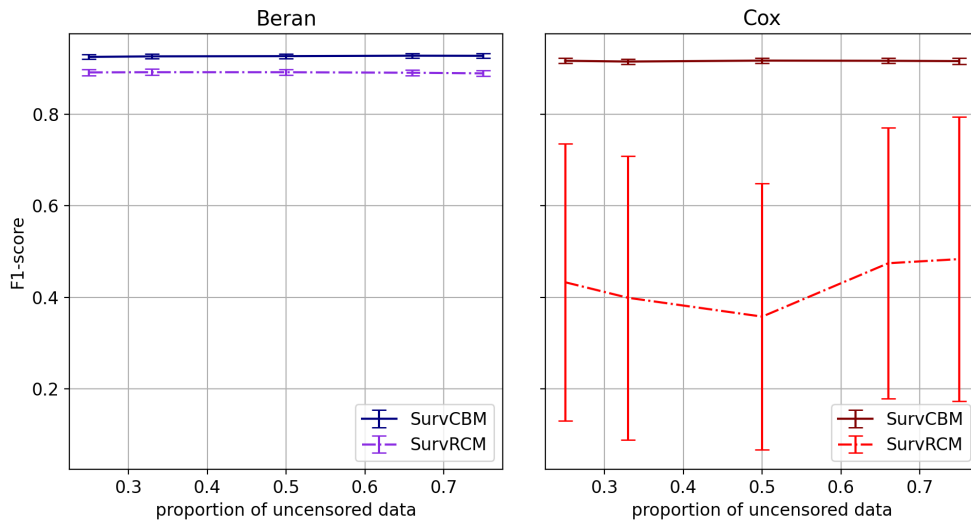


Figure 13: Dependencies of the survival model performance (the F1-measure) on the proportion of uncensored data for the Beran estimator (the left graph) and the Cox model (the right graph) when the MNIST-sin dataset is used

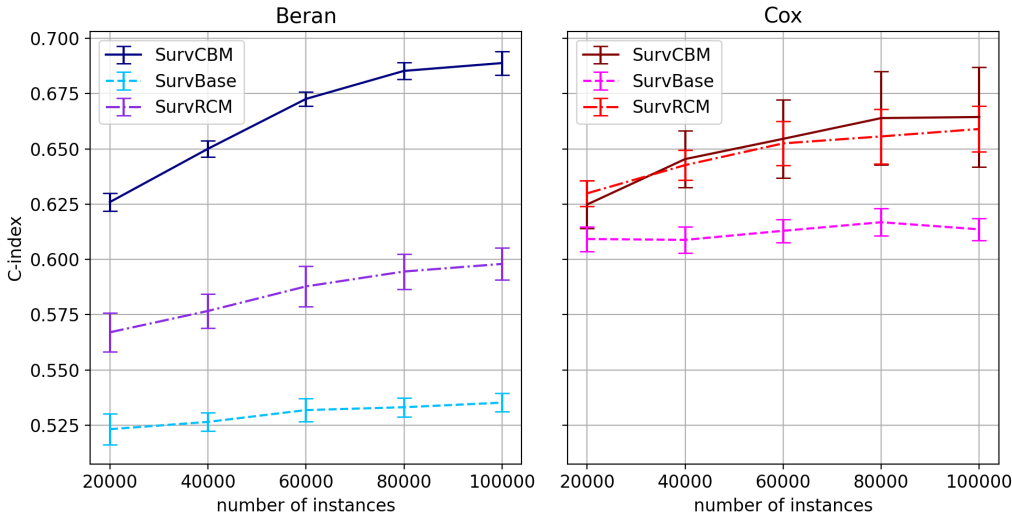


Figure 14: Dependencies of the survival model performance (the C-index) on the number of training instances for the Beran estimator (the left graph) and the Cox model (the right graph) when the CIFAR-10 dataset is used

to generate the event times. At the same time, SurvCBM based on the Beran estimator demonstrates superior results compared to the other models.

The same results are obtained when the F1-measures, as functions of the uncensored data proportion, are studied. These results are shown in Figs. 16 and 17. At first glance, SurvCBM achieves superior results when the Beran estimator is used. However, the absolute values of the accuracy measures are quite low.

6 SurvCBM as an interpretation tool

Depending on the survival model used in SurvCBM, we consider two methods for interpreting predictions which are in the form of SFs.

The first method is applied when the Beran estimator is used in SurvCBM. The goal of this method is to explain which concepts significantly impact the predicted SF $S(t | \mathbf{x})$ for a new instance \mathbf{x} . A key element of this interpretation is the predicted SF itself. However, determining a direct relationship between concepts and the SF is challenging. To address this, the following approach is proposed for interpreting the predicted SF.

The model selects instances from the training set that are closest to the instance being explained in the concept space. Closeness is defined as the distance between the predicted SF of the explainable instance and the SFs of other instances from the

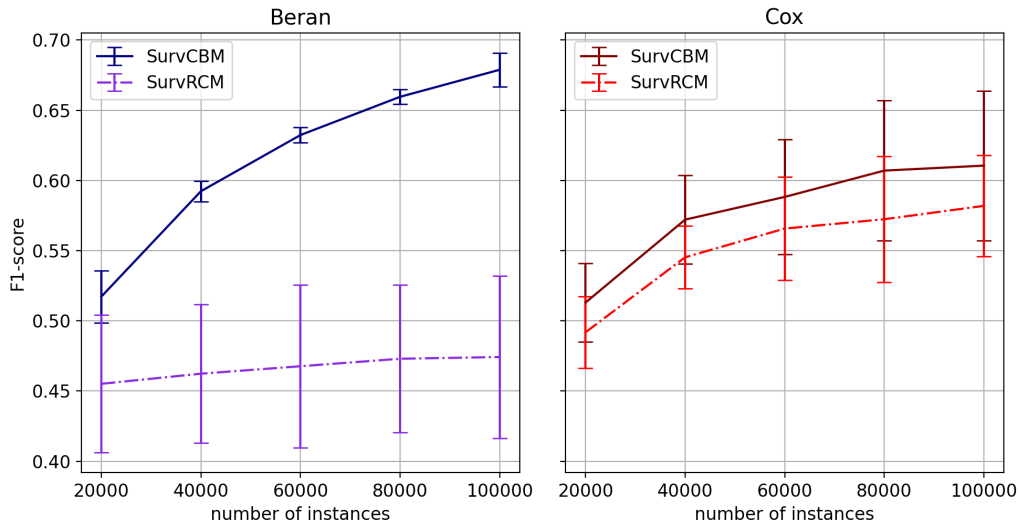


Figure 15: Dependencies of the survival model performance (the F1-measure) on the number of training instances for the Beran estimator (the left graph) and the Cox model (the right graph) when the CIFAR-10 dataset is used

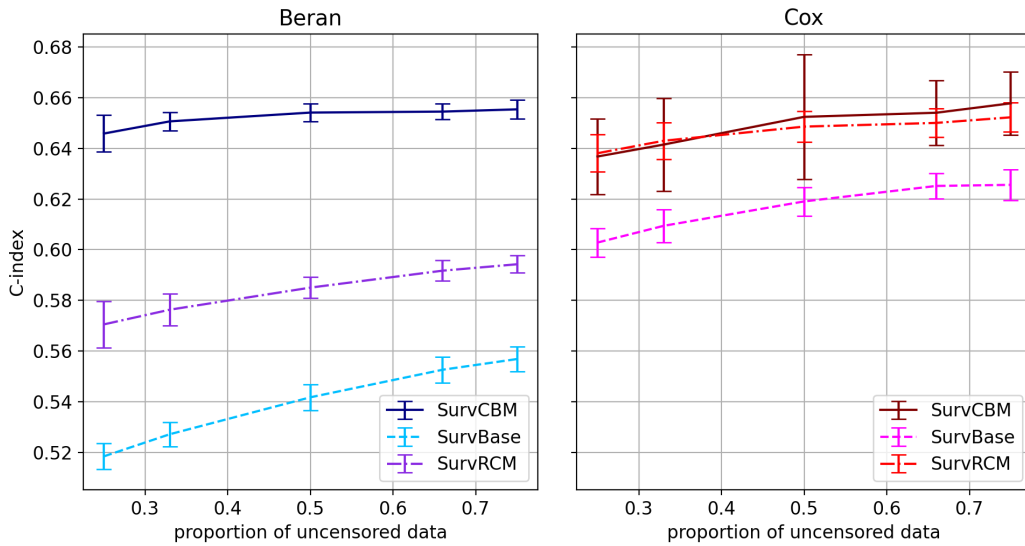


Figure 16: Dependencies of the survival model performance (the C-index) on the proportion of uncensored data for the Beran estimator (the left graph) and the Cox model (the right graph) when the CIFAR-10 dataset is used

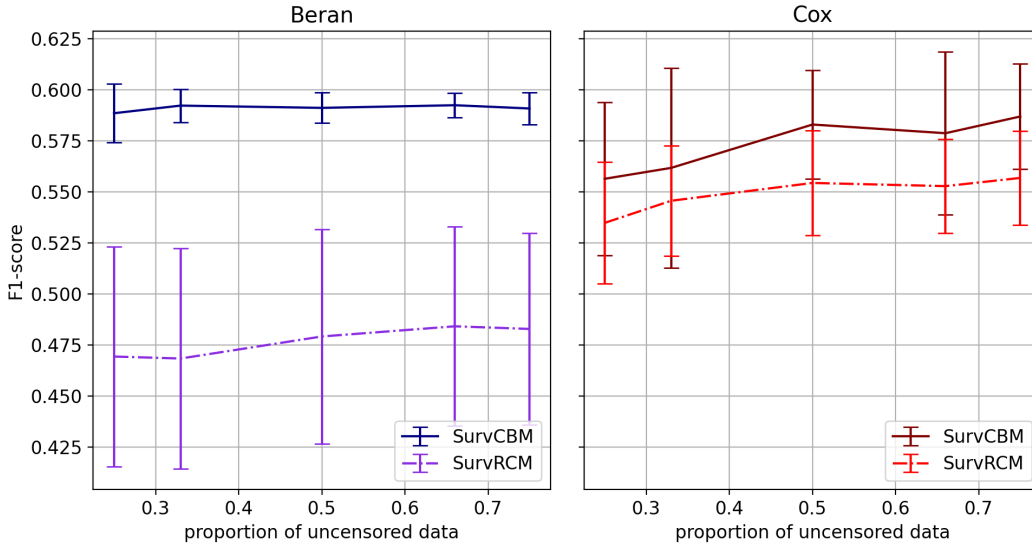


Figure 17: Dependencies of the survival model performance (the F1-measure) on the proportion of uncensored data for the Beran estimator (the left graph) and the Cox model (the right graph) when the CIFAR-10 dataset is used

training data. The number of concepts that coincide with those of the instance being explained, among the nearest instances, determines the degree of importance of these concepts in the prediction corresponding to the explainable example. The more concepts that coincide, the greater their importance. This interpretation can be viewed within the framework of example-based explanations [69].

For the MNIST dataset, the parameters $\mathbf{b} = (\mathbf{b}_1, \mathbf{b}_2, \mathbf{b}_3, \mathbf{b}_4) \in \mathbb{R}^{40}$ in the generation process (13) are set as follows: $\mathbf{b}_1 = (0.5, \dots, 0.5) \in \mathbb{R}^{10}$, $\mathbf{b}_2 = (1.5, \dots, 1.5) \in \mathbb{R}^{10}$, $\mathbf{b}_3 = (0.0001, \dots, 0.0001) \in \mathbb{R}^{10}$, $\mathbf{b}_4 = (0.001, \dots, 0.001) \in \mathbb{R}^{10}$. This indicates that the first and second concepts have significant importance, while the third and fourth concepts are relatively unimportant. Additionally, the parameter values in (13) are set as $\lambda = 10^{-4}$ and $\nu = 2$. For the CIFAR-10 dataset, the parameters $\mathbf{b} = (\mathbf{b}_1, \mathbf{b}_2, \mathbf{b}_3, \mathbf{b}_4) \in \mathbb{R}^{17}$ are defined as: $\mathbf{b}_1 = (0.001, \dots, 0.001) \in \mathbb{R}^5$, $\mathbf{b}_2 = (0.0001, \dots, 0.0001) \in \mathbb{R}^5$, $\mathbf{b}_3 = (3, \dots, 3) \in \mathbb{R}^5$, $\mathbf{b}_4 = (5, 5) \in \mathbb{R}^2$. Here, the third and fourth concepts are important, while the first and second concepts are unimportant. The parameters in (13) are set as $\lambda = 10^{-3}$ and $\nu = 4$.

To improve the classification performance and interpretability of the model, we propose learning the parameter τ of the kernel in the Beran estimator for each value of

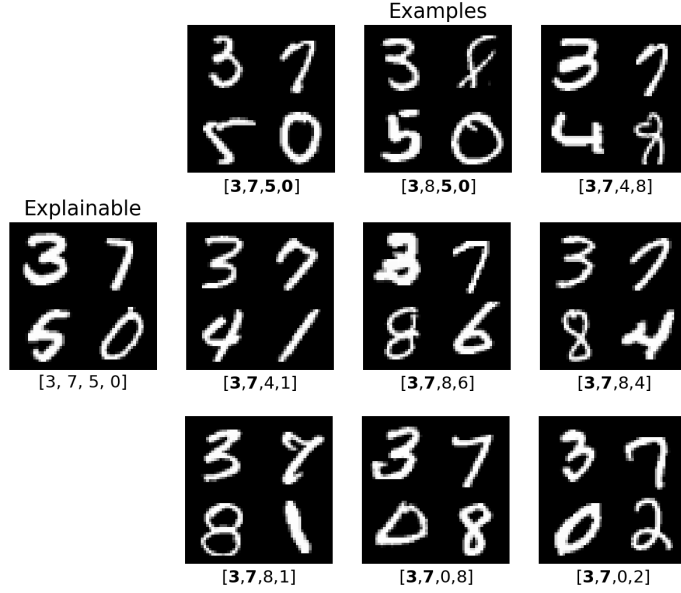


Figure 18: Examples of nearest neighbors for the explainable instance derived from the MNIST dataset based on the Beran estimator

concepts. Weights α in (7) are of the form:

$$\alpha(\mathbf{p}, \mathbf{p}^{(k)}) = \text{softmax} \left(- \sum_{i=1}^m \sum_{j=1}^{k_i} \frac{(p_{i,j} - p_{i,j}^{(k)})^2}{\tau_{i,j}} \right), \quad (15)$$

where $p_{i,j}$ is the j -th value logit of the i -th concept for the explainable instance; $p_{i,j}^{(k)}$ is the j -th value logit of the i -th concept for the k -th instance; $\tau_{i,j}$ is the trainable parameter.

This means that the number of training parameters $\tau_{i,j}$ is equal to M .

Figs. 18 and 19 illustrate examples of nearest instances constructed from the MNIST dataset. In particular, it can be seen from Fig. 18 that the value 3 of the first concept occurs in 9 out of 9 instances, the value 7 of the second concept occurs in 8 instances, the value 5 of the third concept occurs in 2 instances, and the value 0 of the fourth concept occurs in 2 instances. This implies that the first concept is the most important for the prediction of the explainable instance. The second concept is also important, whereas the third and fourth concepts have only a slight impact on the prediction. The similar conclusion can be done by analyzing the example shown in Fig. 19 where the value 8 of the first concept and value 7 of the second concept occur in 7 nearest instances. This implies that the first and the second concepts are the most important.

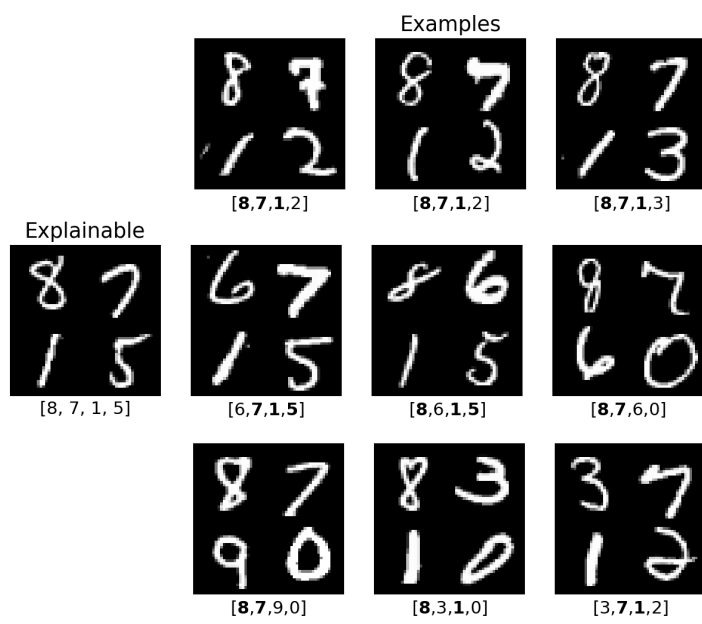


Figure 19: Examples of nearest neighbors for the explainable instance derived from the MNIST dataset based on the Beran estimator



Figure 20: Examples of nearest neighbors for the explainable instance constructed from the CIFAR-10 dataset based on the Beran estimator

Fig. 20 illustrates an example of nearest instances constructed from the CIFAR-10 datasets. It can be clearly seen from Fig. 20 that the value 1 of the third concept and the value 1 of the fourth concept are present in all nearest instances. This indicates that the number of flying objects (the third concept) and the presence of a cat in the image (the fourth concept) are important for explaining the predictions of the explainable instance. Additionally, we observe that all nearest instances share the same values for the first and second concepts. However, these values do not match the corresponding concept values of the explainable instance. Therefore, these concepts are not considered important for the prediction.

The second method is based on the linear relationship underlying the Cox model. Instead of using logits to interpret predictions from the Cox model, we transform the logits into probabilities

$$\pi = (\pi_1, \dots, \pi_m) = (\pi_{i,1}, \dots, \pi_{i,k_i}, i = 1, \dots, m),$$

using the softmax operator. Applying the trained regression coefficients \mathbf{b} from (4) and the probabilities π of the concepts corresponding to the explainable instance, we

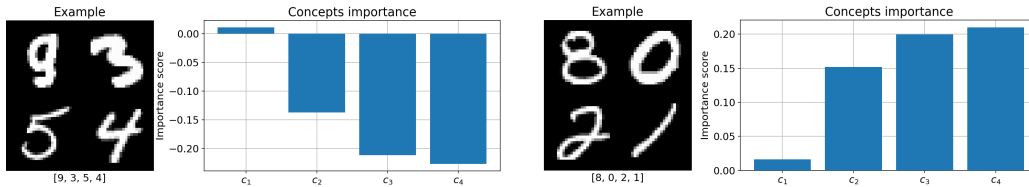


Figure 21: Two examples of the concept importance for explainable instances constructed from the MNIST dataset based on the Cox model

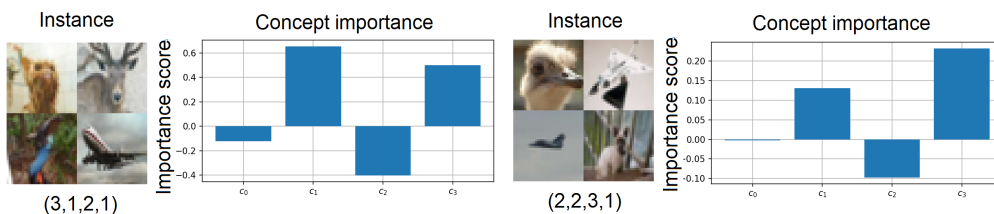


Figure 22: Two examples of the concept importance for explainable instances constructed from the CIFAR-10 dataset based on the Cox model

can determine the importance value of each concept as its contribution into the linear sum $\mathbf{b}^T \pi$. In other words, we compute the product $\mathbf{b}_i^T \pi_i$ to quantify the i -th concept contribution, where \mathbf{b}_i is the i -th part of the vector \mathbf{b} corresponding to the vector $\pi_i = (\pi_{i,1}, \dots, \pi_{i,k_i})$. Figs. 21 and 22 illustrate the explainable instances constructed from the MNIST dataset and from the CIFAR-10 dataset, respectively, along with their concept importance values. It should be noted that the event times are generated in accordance with vectors of coefficients $(0, 7, 10, 14)$ for the MNIST dataset and $(-0.7, 1.5, -2.0, 5.0)$ for the CIFAR-10 dataset.

7 Conclusion

Two concept-based survival learning models have been proposed and compared. Based on numerous numerical experiments and the architectures of the models, SurvCBM outperforms SurvRCM in all cases. Therefore, we focus primarily on the key features of SurvCBM. It is worth noting that the proposed model represents the first attempt to integrate concept-based information into survival analysis. Through extensive numerical experiments, this approach has demonstrated that concept information plays a crucial role in improving both classification and regression accuracy.

SurvCBM is based on a simple implementation of the Beran estimator, which uses

only one training parameter for the Gaussian kernel. A potential extension could involve incorporating additional training parameters into the Beran estimator to enhance its generalization capabilities. Another promising direction is to replace the Beran estimator and the Cox model with neural networks designed to perform the same survival analysis tasks. These modifications represent important avenues for future research.

Another distinctive feature of SurvCBM is its representation of concepts in categorical form. However, it would be valuable to explore concepts that represent time-to-event or other continuous values. This representation is particularly relevant when analyzing the reliability of complex systems composed of multiple components with different reliability characteristics. Such a modification would enable the interpretation of system predictions in terms of unreliable components and could serve as another direction for further research.

The proposed models assume that each instance is described by a set of predefined concepts available a priori. However, in many real-world scenarios, concept information may not be readily available. Therefore, developing approaches to automatically discover concepts from data is an important challenge. While this problem has been addressed in [70], it has not yet been explored within the framework of survival analysis, making it a promising direction for future work.

An important task in many applications, particularly in medicine, is to incorporate expert rules in the form of logical functions of concepts into the learning and inference processes. This approach can be regarded as a combination of inductive and deductive learning in CBL. It has been studied in [71, 72]. However, it can be extended to the case of survival analysis, which represents another promising direction for research.

References

- [1] A. Gupta and P.J. Narayanan. A survey on concept-based approaches for model improvement. arXiv:2403.14566, Mar 2024.
- [2] Been Kim, M. Wattenberg, J. Gilmer, C. Cai, J. Wexler, F. Viegas, et al. Interpretability beyond feature attribution: Quantitative testing with concept activation vectors (tcav). In *International conference on machine learning*, pages 2668–2677. PMLR, 2018.
- [3] I. Lage and F. Doshi-Velez. Learning interpretable concept-based models with human feedback. arXiv:2012.02898, Dec 2020.
- [4] Bowen Wang, Liangzhi Li, Y. Nakashima, and H. Nagahara. Learning bottleneck concepts in image classification. In *Proceedings of the IEEE/CVF Conference on Computer Vision and Pattern Recognition*, pages 10962–10971, 2023.

- [5] Kaiwen Xu, Kazuto Fukuchi, Youhei Akimoto, and Jun Sakuma. Statistically significant concept-based explanation of image classifiers via model knockoffs. In *Proceedings of the Thirty-Second International Joint Conference on Artificial Intelligence*, pages 519–526, 2023.
- [6] Chih-Kuan Yeh, Been Kim, S. Arik, Chun-Liang Li, T. Pfister, and P. Ravikumar. On completeness-aware concept-based explanations in deep neural networks. In *Advances in neural information processing systems*, volume 33, pages 20554–20565, 2020.
- [7] R. Guidotti, A. Monreale, S. Ruggieri, F. Turini, F. Giannotti, and D. Pedreschi. A survey of methods for explaining black box models. *ACM computing surveys*, 51(5):93, 2019.
- [8] Y. Liang, S. Li, C. Yan, M. Li, and C. Jiang. Explaining the black-box model: A survey of local interpretation methods for deep neural networks. *Neurocomputing*, 419:168–182, 2021.
- [9] Yu Zhang, Peter Tiño, Aleš Leonardis, and Ke Tang. A survey on neural network interpretability. *IEEE Transactions on Emerging Topics in Computational Intelligence*, 5(5):726–742, 2021.
- [10] E. Poeta, G. Ciravegna, E. Pastor, T. Cerquitelli, and E. Baralis. Concept-based explainable artificial intelligence: A survey. arXiv:2312.12936, May 2023.
- [11] Lijie Hu, Chenyang Ren, Zhengyu Hu, Cheng-Long Wang, and Di Wang. Editable concept bottleneck models. arXiv:2405.15476, May 2024.
- [12] Pang Wei Koh, Thao Nguyen, Yew Siang Tang, S. Mussmann, E. Pierson, Been Kim, and Percy Liang. Concept bottleneck models. In *International conference on machine learning*, pages 5338–5348. PMLR, 2020.
- [13] K. Chauhan, R. Tiwari, J. Freyberg, P. Shenoy, and K. Dvijotham. Interactive concept bottleneck models. In *Proceedings of the AAAI Conference on Artificial Intelligence*, volume 37, pages 5948–5955, 2023.
- [14] A. Sarkar, D. Vijaykeerthy, A. Sarkar, and V.N. Balasubramanian. A framework for learning ante-hoc explainable models via concepts. In *Proceedings of the IEEE/CVF Conference on Computer Vision and Pattern Recognition (CVPR)*, pages 10286–10295, June 2022.
- [15] Eunji Kim, Dahuin Jung, Sangha Park, Siwon Kim, and Sungroh Yoon. Probabilistic concept bottleneck models. In *International Conference on Machine Learning*, pages 16521–16540. PMLR, 2023.

- [16] A.A. Ismail, J. Adebayo, H.C. Bravo, S. Ra, and Kyunghyun Cho. Concept bottleneck generative models. In *Proceedings of ICML 2023. Workshop on Deployment Challenges for Generative AI*, pages 1–10, 2023.
- [17] R. Kazmierczak, E. Berthier, G. Frehse, and G. Franchi. CLIP-QDA: An explainable concept bottleneck model. *Transactions on Machine Learning Research*, 2024.
- [18] E. Marconato, A. Passerini, and S. Teso. Glancenets: Interpretable, leak-proof concept-based models. In *Advances in Neural Information Processing Systems*, volume 35, pages 21212–21227, 2022.
- [19] M. Vandenhirtz, S. Laguna, R. Marcinkevičs, and J.E. Vogt. Stochastic concept bottleneck models. In *ICML 2024 Workshop on Structured Probabilistic Inference & Generative Modeling*, 2024.
- [20] M.E. Zarlenga, Z. Shams, M.E. Nelson, B. Kim, and M. Jamnik. TabCBM: Concept-based interpretable neural networks for tabular data. *Transactions on Machine Learning Research*, 2023.
- [21] D. Hosmer, S. Lemeshow, and S. May. *Applied Survival Analysis: Regression Modeling of Time to Event Data*. John Wiley & Sons, New Jersey, 2008.
- [22] F. Forest, K. Rombach, and O. Fink. Interpretable prognostics with concept bottleneck models. arXiv:2405.17575, May 2024.
- [23] D.R. Cox. Regression models and life-tables. *Journal of the Royal Statistical Society, Series B (Methodological)*, 34(2):187–220, 1972.
- [24] M.S. Kovalev, L.V. Utkin, and E.M. Kasimov. SurvLIME: A method for explaining machine learning survival models. *Knowledge-Based Systems*, 203:106164, 2020.
- [25] R. Beran. Nonparametric regression with randomly censored survival data. Technical report, University of California, Berkeley, 1981.
- [26] L.V. Utkin, D.Y. Eremenko, and A.V. Konstantinov. SurvBeX: an explanation method of the machine learning survival models based on the beran estimator. *International Journal of Data Science and Analytics*, pages 1–26, 2024.
- [27] Ivaxi Sheth and Samira Ebrahimi Kahou. Auxiliary losses for learning generalizable concept-based models. *Advances in Neural Information Processing Systems*, 36, 2024.
- [28] Lijie Hu, Tianhao Huang, Huanyi Xie, Chenyang Ren, Zhengyu Hu, Lu Yu, and Di Wang. Semi-supervised concept bottleneck models. arXiv:2406.18992, Jun 2024.

- [29] T. Oikarinen, S. Das, L.M. Nguyen, and Tsui-Wei Weng. Label-free concept bottleneck models. arXiv:2304.06129, Apr 2023.
- [30] Hongmei Wang, Junlin Hou, and Hao Chen. Concept complement bottleneck model for interpretable medical image diagnosis. arXiv:2410.15446, Oct 2024.
- [31] S. Schrodi, J. Schur, M. Argus, and T. Brox. Concept bottleneck models without predefined concepts. arXiv:2407.03921, Jul 2024.
- [32] Mert Yuksekgonul, Maggie Wang, and James Zou. Post-hoc concept bottleneck models. In *ICLR 2022 Workshop on PAIR* *{\textasciicircum} 2Struct: Privacy, Accountability, Interpretability, Robustness, Reasoning on Structured Data*, 2022.
- [33] Chenming Shang, Shiji Zhou, Hengyuan Zhang, Xinzhe Ni, Yujiu Yang, and Yuwang Wang. Incremental residual concept bottleneck models. In *Proceedings of the IEEE/CVF Conference on Computer Vision and Pattern Recognition*, pages 11030–11040, 2024.
- [34] Gabriele Dominici, Pietro Barbiero, Francesco Giannini, Martin Gjoreski, and Marc Langhenrich. AnyCBMs: How to turn any black box into a concept bottleneck model. arXiv:2405.16508, May 2024.
- [35] H.I. Aysel, Xiaohao Cai, and A. Prugel-Bennett. Concept-based explainable artificial intelligence: Metrics and benchmarks. arXiv:2501.19271, Jan 2025.
- [36] Jae Hee Lee, S. Lanza, and S. Wermter. From neural activations to concepts: A survey on explaining concepts in neural networks. arXiv:2310.11884, Oct 2023.
- [37] A. Mahinpei, J. Clark, I. Lage, F. Doshi-Velez, and Weiwei Pan. Promises and pitfalls of black-box concept learning models. arXiv:2106.13314, Jun 2021.
- [38] P. Wang, Y. Li, and C.K. Reddy. Machine learning for survival analysis: A survey. *ACM Computing Surveys (CSUR)*, 51(6):1–36, 2019.
- [39] Stephen Salerno and Yi Li. High-dimensional survival analysis: Methods and applications. *Annual review of statistics and its application*, 10:25–49, 2023.
- [40] Simon Wiegrebe, Philipp Kopper, Raphael Sonabend, Bernd Bischl, and Andreas Bender. Deep learning for survival analysis: a review. *Artificial Intelligence Review*, 57(65):1–34, 2024.
- [41] G.H. Chen. An introduction to deep survival analysis models for predicting time-to-event outcomes. *Foundations and Trends® in Machine Learning*, 17(6):921–1100, 2024.

- [42] F. Emmert-Streib and M. Dehmer. Introduction to survival analysis in practice. *Machine Learning & Knowledge Extraction*, 1:1013–1038, 2019.
- [43] J.L. Katzman, U. Shaham, A. Cloninger, J. Bates, T. Jiang, and Y. Kluger. Deep-surv: Personalized treatment recommender system using a Cox proportional hazards deep neural network. *BMC medical research methodology*, 18(24):1–12, 2018.
- [44] M. Luck, T. Sylvain, H. Cardinal, A. Lodi, and Y. Bengio. Deep learning for patient-specific kidney graft survival analysis. arXiv:1705.10245, May 2017.
- [45] M.Z. Nezhad, N. Sadati, K. Yang, and D. Zhu. A deep active survival analysis approach for precision treatment recommendations: Application of prostate cancer. arXiv:1804.03280v1, April 2018.
- [46] Kan Ren, Jiarui Qin, Lei Zheng, Zhengyu Yang, Weinan Zhang, Lin Qiu, and Yong Yu. Deep recurrent survival analysis. In *Proceedings of the AAAI conference on artificial intelligence*, volume 33, pages 4798–4805, 2019.
- [47] J.A. Steingrimsdóttir and S. Morrison. Deep learning for survival outcomes. *Statistics in Medicine*, 39(17):2339–2349, 2020.
- [48] A. Tarkhan, N. Simon, T. Bengtsson, K. Nguyen, and J. Dai. Survival prediction using deep learning. In *Proceedings of AAAI Spring Symposium on Survival Prediction-Algorithms, Challenges and Applications*, volume 146, pages 207–214. PMLR, 2021.
- [49] J. Yao, X. Zhu, F. Zhu, and J. Huang. Deep correlational learning for survival prediction from multi-modality data. In *Medical Image Computing and Computer-Assisted Intervention – MICCAI 2017*, volume 10434 of *Lecture Notes in Computer Science*, pages 406–414. Springer, Cham, 2017.
- [50] Qixian Zhong, J.W. Mueller, and Jane-Ling Wang. Deep extended hazard models for survival analysis. In *Advances in Neural Information Processing Systems*, volume 34, pages 15111–15124. Curran Associates, Inc., 2021.
- [51] Prayag Chatha, Yixin Wang, Zhenke Wu, and J. Regier. Dynamic survival transformers for causal inference with electronic health records. arXiv:2210.15417, Oct. 2022.
- [52] Shi Hu, Egill Fridgeirsson, Guido van Wingen, and Max Welling. Transformer-based deep survival analysis. In *Survival Prediction-Algorithms, Challenges and Applications*, pages 132–148. PMLR, 2021.

- [53] Chunyuan Li, Xinliang Zhu, Jiawen Yao, and Junzhou Huang. Hierarchical transformer for survival prediction using multimodality whole slide images and genomics. In *The 26th International Conference on Pattern Recognition (ICPR)*, pages 4256–4262. IEEE Computer Society, 2022.
- [54] Zhilong Lv, Yuexiao Lin, Rui Yan, Ying Wang, and Fa Zhang. Transsurv: Transformer-based survival analysis model integrating histopathological images and genomic data for colorectal cancer. *IEEE/ACM Transactions on Computational Biology and Bioinformatics*, pages 1–10, 2022.
- [55] Yifan Shen, Li liu, Zhihao Tang, Zongyi Chen, Guixiang Ma, Jiyan Dong, Xi Zhang, Lin Yang, and Qingfeng Zheng. Explainable survival analysis with convolution-involved vision transformer. In *Proceedings of the AAAI Conference on Artificial Intelligence (AAAI-22)*, volume 36, pages 2207–2215, 2022.
- [56] Zhihao Tang, Li Liu, Zongyi Chen, Guixiang Ma, Jiyan Dong, Xujie Sun, Xi Zhang, Chaozhuo Li, Qingfeng Zheng, Lin Yang, et al. Explainable survival analysis with uncertainty using convolution-involved vision transformer. *Computerized Medical Imaging and Graphics*, 110:102302, 2023.
- [57] Zifeng Wang and Jimeng Sun. Survtrace: Transformers for survival analysis with competing events. In *Proceedings of the 13th ACM International Conference on Bioinformatics, Computational Biology and Health Informatics*, pages 1–9, 2022.
- [58] Xingyu Li, V. Krivtsov, and K. Arora. Attention-based deep survival model for time series data. *Reliability Engineering and System Safety*, 217(108033):1–12, 2022.
- [59] Zhaohong Sun, Wei Dong, Jinlong Shi, Kunlun He, and Zhengxing Huang. Attention-based deep recurrent model for survival prediction. *ACM Transactions on Computing for Healthcare*, 2(4):1–18, 2021.
- [60] N.A. Ibrahim, A. Kudus, I. Daud, and M.R. Abu Bakar. Decision tree for competing risks survival probability in breast cancer study. *International Journal Of Biological and Medical Research*, 3(1):25–29, 2008.
- [61] M.N. Wright, T. Dankowski, and A. Ziegler. Unbiased split variable selection for random survival forests using maximally selected rank statistics. *Statistics in Medicine*, 36(8):1272–1284, 2017.
- [62] C. Haarburger, P. Weitz, O. Rippel, and D. Merhof. Image-based survival analysis for lung cancer patients using CNNs. arXiv:1808.09679v1, Aug 2018.

- [63] A. Widodo and B.-S. Yang. Machine health prognostics using survival probability and support vector machine. *Expert Systems with Applications*, 38(7):8430–8437, 2011.
- [64] D.M. Witten and R. Tibshirani. Survival analysis with high-dimensional covariates. *Statistical Methods in Medical Research*, 19(1):29–51, 2010.
- [65] F. Harrell, R. Califf, D. Pryor, K. Lee, and R. Rosati. Evaluating the yield of medical tests. *Journal of the American Medical Association*, 247:2543–2546, 1982.
- [66] H. Uno, Tianxi Cai, M.J. Pencina, R.B. D’Agostino, and Lee-Jen Wei. On the c-statistics for evaluating overall adequacy of risk prediction procedures with censored survival data. *Statistics in medicine*, 30(10):1105–1117, 2011.
- [67] Y. LeCun, L. Bottou, Y. Bengio, and P. Haffner. Gradient-based learning applied to document recognition. *Proceedings of the IEEE*, 86(11):2278–2324, 1998.
- [68] A. Krizhevsky and G. Hinton. Learning multiple layers of features from tiny images. Technical Report 1, Computer Science Department, University of Toronto, 2009.
- [69] A. Poché, L. Hervier, and M.-C. Bakkay. Natural example-based explainability: a survey. In *World Conference on eXplainable Artificial Intelligence*, pages 24–47. Springer, 2023.
- [70] S.S. Rao, S. Mahajan, M. Böhle, and B. Schiele. Discover-then-name: Task-agnostic concept bottlenecks via automated concept discovery. In *18th European Conference on Computer Vision*, pages 444–461. Springer, 2024.
- [71] A.V. Konstantinov and L.V. Utkin. An explicit concept-based approach for incorporating expert rules into machine learning models. In *Proceedings of the Eighth International Scientific Conference Intelligent Information Technologies for Industry (IITI’24)*, volume 1 of *Lecture Notes in Networks and Systems*, vol. 1209, pages 153–162. Springer, Cham, 2024.
- [72] A.V. Konstantinov and L.V. Utkin. Incorporating expert rules into neural networks in the framework of concept-based learning. arXiv:2402.14726, Feb 2024.